Analytical and Bioanalytical Chemistry (2018) 410:6663–6676
https://doi.org/10.1007/s00216-018-1279-0

RESEARCH PAPER

Optimization, performance, and application of a pyrolysis-GC/MS method for the identification of microplastics

Ludovic Hermabessiere[1] · Charlotte Himber[1] · Béatrice Boricaud[1] · Maria Kazour[2,3] · Rachid Amara[2] · Anne-Laure Cassone[4] · Michel Laurentie[5] · Ika Paul-Pont[4] · Philippe Soudant[4] · Alexandre Dehaut[1] · Guillaume Duflos[1]

Received: 7 May 2018 / Revised: 26 June 2018 / Accepted: 17 July 2018 / Published online: 27 July 2018

Abstract

Plastics are found to be major debris composing marine litter; microplastics (MP, < 5 mm) are found in all marine compartments. The amount of MPs tends to increase with decreasing size leading to a potential misidentification when only visual identification is performed. These last years, pyrolysis coupled with gas chromatography/mass spectrometry (Py-GC/MS) has been used to get information on the composition of polymers with some applications on MP identification. The purpose of this work was to optimize and then validate a Py-GC/MS method, determine limit of detection (LOD) for eight common polymers, and apply this method on environmental MP. Optimization on multiple GC parameters was carried out using polyethylene (PE) and polystyrene (PS) microspheres. The optimized Py-GC/MS method require a pyrolysis temperature of 700 °C, a split ratio of 5 and 300 °C as injector temperature. Performance assessment was accomplished by performing repeatability and intermediate precision tests and calculating limit of detection (LOD) for common polymers. LODs were all below 1 μg. For performance assessment, identification remains accurate despite a decrease in signal over time. A comparison between identifications performed with Raman micro spectroscopy and with Py-GC/MS was assessed. Finally, the optimized method was applied to environmental samples, including plastics isolated from sea water surface, beach sediments, and organisms collected in the marine environment. The present method is complementary to μ-Raman spectroscopy as Py-GC/MS identified pigment containing particles as plastic. Moreover, some fibers and all particles from sediment and sea surface were identified as plastic.

Keywords Microplastics · Pyrolysis · Gas chromatography · Method · Environmental samples

Alexandre Dehaut and Guillaume Duflos contributed equally to this work.

Electronic supplementary material The online version of this article (https://doi.org/10.1007/s00216-018-1279-0) contains supplementary material, which is available to authorized users.

✉ Guillaume Duflos
guillaume.duflos@anses.fr

[1] ANSES, Laboratoire de Sécurité des Aliments, Boulevard du Bassin Napoléon, 62200 Boulogne, France

[2] UMR 8187, LOG, Laboratoire d'Océanologie et de Géosciences, CNRS, University of Littoral Côte d'Opale, University of Lille, 32 Avenue Foch, 62930 Wimereux, France

[3] CNRS, National Centre for Marine Sciences, PO Box 534, Batroun, Lebanon

[4] Laboratoire des Sciences de l'Environnement Marin (LEMAR), UMR6539/UBO/CNRS/IRD/IFREMER, Technopôle Brest-Iroise, Institut Universitaire Européen de la Mer, rue Dumont d'Urville, 29280 Plouzané, France

[5] ANSES, Plateforme PAS, Laboratoire de Fougères, 10 B rue Claude Bourgelat, Javené, 35300 Fougères, France

Introduction

Plastic is a commonly used material as it is inexpensive, strong, lightweight, and easy to manufacture [1]. Plastic production increased from the 1950s and reached 335 million metric tons in 2016 [2]. Due to waste management issues and incivilities, it has been estimated that 5 to 12 million plastic particles end up in oceans in 2010 [3]. Low estimates predicted that floating marine plastic weight between 70,000 and 270,000 tons [4–6], thus, potentially representing more than 51 trillion plastic pieces in oceans [6].

Microplastics (MP) are plastic particles smaller than 5 mm in their longest size [7]. To date, multiple studies are carried out to quantify MP in sediments, in water column, and in organisms from both freshwater and marine environments [8, 9]. For large MP (1–5 mm) [10] and macroplastic (> 5 mm), visual identification relying on physical characteristics is possible but the proportion of misidentification grows with

decreasing particles size [11]. However, some studies still do not perform any characterization of MP based on their chemical composition [12]. Additionally, as plastic materials include a large variety of polymers, more than 5000 grades [13], chemical identification is now mandatory to ensure the accuracy of collected pollution data [14]. Raman and Fourier transform infrared (FTIR) spectroscopies are the most common techniques employed to identify polymer types of MP [15]. Furthermore, the use of imaging techniques coupled to spectroscopic approaches allows automatization of MP identification [16–18]. In addition to spectroscopic methods, another type of chemical identification is thermal analysis [12]. Pyrolysis-gas chromatography coupled with mass spectrometry (Py-GC/MS) is one of the thermal analysis techniques used to identify MP polymers. Py-GC/MS has been used to identify MP from different matrix based on their thermal degradation products [19–25]. Furthermore, Py-GC/MS allows the analysis of a whole MP particle in contrast with Raman or FTIR (in reflection mode) which only analyze the surface of the MP particle being sensitive to interference caused by additives such as pigments [26–28], for example.

To date, studies using Py-GC/MS to identify the polymeric composition of MP document neither the method development nor the assessment of its performance. Some authors stated that Py-GC/MS is only feasible with MP > 500 μm [29, 30] even if so far, 100 μm is the smallest size of an isolated MP that has been identified [19]. Recently, particles smaller than 1 μm, referred as nanoplastics by the authors, have been identified as plastics based on Py-GC/MS and statistical approaches in bulk samples from the North Atlantic Subtropical Gyre [31].

The purpose of this work was fourfolds: (i) optimize a Py-GC/MS method to accurately identify polymer of MP, (ii) assess the performance of the Py-GC/MS approach, (iii) compare identifications with samples already identified by μ-Raman, and (iv) apply this technique to environmental samples.

Material and methods

Reference material

Microspheres with calibrated size ranges were purchased for the Py-GC/MS optimization method. Polyethylene (PE) (180–212 μm; reference: CPMS-0.96180-212um) and poly(methyl methacrylate) (PMMA) (180–212 μm; reference: PMMAMS-1.2180-212um) microspheres were acquired from Cospheric LLC (Santa Barbara, USA) and polystyrene (PS) (106–125 μm; reference: 198241) from Polysciences Europe GmbH (Hirschberg an der Bergstrasse, Germany). For the calculation of the LOD, other polymers were bought from Goodfellow (Lille, France) including filaments of polycaprolactam (PA-6), polyethylene terephthalate (PET), and polypropylene (PP) and fragments of polycarbonate (PC) and unplasticized polyvinyl chloride (uPVC).

For all polymers, characteristic compounds are presented in Table 1 (see Electronic Supplementary Material (ESM) Figs. S1 to S8) and were choose according to their representativeness for polymer identification, their relative intensity, and in comparison with the literature [22, 32, 33].

Sample preparation

Each particle was selected based on its size (ca. 200 μm) under a SZ61 stereomicroscope (Olympus, Rungis, France) and then introduced into an analysis cup (Frontier-Lab, Fukushima, Japan) for Py-GC/MS analysis. All analysis cup used in this work were brand new cups visually controlled prior to analysis to detect any possible contamination.

Size and weight estimation

In order to estimate the size of the particle, a photograph was taken with a scale bar using a DP21 camera (Olympus, Rungis, France) mounted on the stereomicroscope. The size in pixel of the particle was recorded using GIMP 2 software (2.8.16). Then, the maximum size in micrometers of the particle was calculated using the scale bar. For each particle, the volume (cm^3) was estimated using different formulas (1), (2), or (3), where D corresponds to the diameter, L to the length, and S to the side size (see ESM, weight estimation). The volume was then multiplied by the density (g/cm^3) of the polymer to obtain the estimated weight.

$$Microsphere\ volume = \frac{4}{3} \times \pi \times \left(\frac{D}{2}\right)^3 \quad (1)$$

$$Filament\ volume = \left(\frac{D}{2}\right)^2 \times \pi \times L \quad (2)$$

$$Fragment\ volume = S^2 \times L \quad (3)$$

Method optimization

Initial Py-GC/MS method

The hereafter called "initial method" was described by Dehaut et al. [35]. Briefly, the analysis cup containing the plastic was placed on the AS-1020E autosampler of an EGA/PY-3030D device (Frontier Lab, Fukushima, Japan). Samples were pyrolyzed at 600 °C for 1 min. Pyrolysis products were injected with a split of 20, on a GC-2010 device (Shimadzu, Noisiel, France) equipped by a RXi-5 ms® column (60 m, 0.25 mm, 25 μm thickness) (Restek, Lisses, France). Temperatures of the pyrolyzer interface and the injection port were both set at

Table 1 Polymer-related pyrogram information

Polymer	Characteristic compound[a]	LRI[b]	Indicator ion (m/z)
PE	1-Nonene (C9)	893	83; 97
	1-Decene (C10)	993	83; 97
	1-Undecene (C11)	1093	83; 97
	1-Dodecene (C12)	1192	83; 97
	1-Tridecene (C13)	1292	83; 97
	1-Tetradecene (C14)	1392	83; 97
	1-Pentadecene (C15)	1492	83; 97
	1-Hexadecene (C16)	1578	83; 97
PS	*Styrene*	898	78; 104
	3-butene-1,3-diyldibenzene (styrene dimer)	1733	91; 208
PMMA	*Methyl methacrylate*	743	41; 69; 100
PP	*2,4-dimethyl-1-heptene*	846	70
PA-6	*ε-caprolactam*	1274	113
PC	Phenol	980	66; 94
	p-Cresol	1075	77; 107
	p-Ethylphenol	1168	107; 122
	p-Vinylphenol	1217	91; 120
	p-Isopropenylphenol	1304	119; 134
	Bisphenol A	2088	213; 228
PET	Benzene	770	52; 78
	Acetophenone	1076	51; 77; 105
	Vinyl benzoate	1145	52; 77; 105
	Benzoic acid	1178	77; 105; 122
	Divinyl terephthalate	1574	104; 175
uPVC	Benzene	770	52; 78
	Toluene	782	91
	Styrene	898	78; 104
	Indene	1059	116
	Naphthalene	1206	128
	2-methylnaphthalene	1320	115; 142
	1-methylnaphthalene	1340	115; 142

[a] Marker compounds in italics were used to calculate limit of detection

[b] Retention index was calculated according to van Den Dool and Kratz [34]; m/z: mass to charge ratio

300 °C. Helium was used as a carrier gas with a linear velocity of 40 cm/s. The initial oven program, called here after *program 0*, was set as follows: 40 °C for 2 min, then increase to 320 °C at 20 °C/min, maintained for 14 min. Mass spectra were obtained by a Shimadzu QP2010-Plus mass spectrometer. Interface temperature was set at 300 °C, ion source temperature was set at 200 °C, ionization voltage was set at 70 eV, and a mass range from 33 to 500 m/z was scanned at 2000 Hz.

As a primary attempt, polymer identification was realized using total ion pyrogram (TIC) which was firstly identified using F-Search software 4.3, querying pyrograms against Frontier Lab's database, and our own database containing pre-established pyrograms with plastic samples. Identification was established based on the similarity percentage (minimum value of 80%) between average mass spectra on the whole chromatogram. Our home-made database was created using our "'initial method" and the optimized Py-GC/MS method on plastic references from Goodfellow (Lille, France). Plastic references used for our home-made database included PE, PS, PP, PET, PA-6, PC, PMMA, and uPVC.

When identification was not possible after primary attempt, a classical GC/MS treatment was performed. Peaks of pyrograms were integrated and compared with available literature [32] or characteristic compounds (Table 1), single peak identification being carried out using NIST08 database and LRI.

Pyrolysis temperature

Optimization of the pyrolysis temperature was carried out using the initial pyrolysis method. The impact of pyrolysis

temperature was determined using five replicate of PE microspheres. Three additional pyrolysis temperatures were tested: 500, 700, and 800 °C for 1 min.

GC oven temperature program

In addition to *program 0*, two others temperature programs were tested. *Program 1* was set as follows: 40 °C for 2 min, then increase to 200 °C at 15 °C/min followed by a second increase to 300 °C at 10 °C/min maintained for 2 min. *Program 2* was set as follows: 40 °C for 2 min, then increase to 261 °C at 13 °C/min followed by a second increase to 300 °C at 6 °C/min maintained for 2 min. Except pyrolysis temperature was set at 700 °C the optimal temperature for 1 min (cf. 0), oven program was the unique parameter modified in this part; other parameters were conserved as those of the initial method. The impact of GC oven temperature program on resolution was determined using PE microspheres. Here, the resolution was only used to assess the separation between PE alkene and alkadiene. The resolution of alkenes (from C_9 to C_{16}) was used to evaluate each program performance. Resolution was calculated by the Shimadzu GC-MS postrun analysis software using (4), where T_r corresponds to the retention time of the considered peak (Alkene), T_{rp} to the retention time of the previous peak (Alkadiene), W to the width of the considered peak, and W_p to the width of the previous peak:

$$Resolution = 2 \times \frac{T_r - T_{rp}}{W + W_p} \quad (4)$$

Five replicates were performed per program.

Injector temperature and split ratio

Optimization on the split ratio and injector temperature was performed using PE and PS microspheres. Here, PS was used in addition to PE as this polymer exhibits only a few degradation products after pyrolysis (Table 1). Three split ratios (50, 20, and 5) and three injector temperatures (280, 300, and 320 °C) were applied, resulting in nine distinct combinations. For all combinations, pyrolysis temperature and GC oven program were set following the previous optimization steps; other parameters were conserved as those described for the initial method (cf. 0). For each combination, five microspheres of PE and PS were analyzed.

Method performance evaluation

Split ratios were adjusted to ensure that no saturation of the mass spectrum occurred. To do so, split ratio was set at 5 for PE microspheres, particles identified by μ-Raman spectroscopy, and unknown particles injection, whereas for PMMA and PS microspheres injection, a split of 50 was chosen.

Repeatability and intermediate precision

For repeatability and intermediate precision, respectively ten and five microspheres of the three polymers were pyrolyzed and the relative standard deviation (RSD) (5) was calculated for each characteristic peak according to ISO 5725-3 [36] where s is the standard deviation and m is the mean:

$$RSD\ (\%) = \frac{s}{m} \times 100 \quad (5)$$

Intermediate precision was assessed over time with pyrolysis occurring at 3, 4, and 6 weeks after repeatability experiences. The method is considered valid if RSD is below 20% for repeatability and intermediate precision. Moreover, polymer identification of the particles was performed as previously described (cf. 0) to obtain qualitative data.

Limit of detection

Limit of detection was calculated according to Caporal-Gautier et al. [37]. First, ten analysis cups without plastic, hereafter referred as "blank," were pyrolyzed. For each blank and at the retention time of each characteristic peak of the eight used polymers (Table 1), the maximum height was determined over a time interval equal to 20 times the full width at half maximum (FWHM); this area is called H_{20FWHM}. Interval surrounds the retention time of each peak with the retention time being the central point of the time range. Five particles were pyrolyzed for each polymer. A response factor (R) (6) was calculated: "Weight" corresponds to the mean the average calculated weight and "height" corresponds to the mean height of the characteristic peak for the five particles:

$$Response\ factor\ (R) = \frac{Weight}{Height} \quad (6)$$

Finally, for each polymer, LOD was calculated as follows:

$$Limit\ of\ Detection\ (LOD) = 3 \times R \times H_{20FWHM} \quad (7)$$

Method comparison

Sampling

Unknown plastic particles were first analyzed by μ-Raman and then by Py-GC/MS before identification to be compared. Comparison of the identification of unknown plastic particles obtained after μ-Raman spectroscopy and Py-GC/MS was performed. To assess methods

comparison, 50 plastic particles hand sampled on a local beach (Equihen Plage, France—50° 39′ 51.08″ N, 1° 34′ 17.94″ E) were used.

Identification by μ-Raman and Py-GC/MS

For μ-Raman analysis, each particle was analyzed with an XploRA PLUS V1.2 (HORIBA Scientific, France SAS) equipped with two lasers of 785- and 532-nm wavelength. First, plastic particles were analyzed with laser wavelength set at 785 nm over a range of 50 to 3940 cm^{-1} with a × 10 (NA = 0.25; WD = 10.6 mm) or × 100 (NA = 0.9; WD = 0.21 mm) objective (Olympus, France). If identification with the 785 nm laser was not successful, particles were secondly analyzed with a laser wavelength set at 532 nm over a range of 50 to 4000 cm^{-1} with a × 10 or × 100 objective. The experimental conditions (integration time, accumulation, laser power) were adapted to limit fluorescence and increase the spectral quality of the analyzed particles. Polymer identification was carried out using spectroscopy software (KnowItAll, Bio-Rad) and our own database containing pre-established polymers spectra. Identification was considered correct if Hit Quality Index (HQI) was above 80 (ranging from 0 to 100). If identification of a particle was not successful after μ-Raman spectroscopy, the particle was then included in the section 0.

For Py-GC/MS, a piece of each particle was cut to the smallest possible size and prepared as indicated in section 0. Pyrolysis-GC/MS was realized as described above (cf. 0).

Application: identification of unknown particles

Sampling

Application of the Py-GC/MS was performed using particles collected on a beach, extracted from bivalves and collected on sea surface waters.

Ten particles, collected by hand on a local beach, including 4 particles identified as pigment and 6 particles unidentified (cf. 0) were analyzed using Py-GC/MS.

Mussels (*Mytilus edulis*) and cockles (*Cerastoderma edule*) were respectively sampled during morning low tides at Le Portel, France (50° 42′ 30.02″ N, 1° 33′ 34.43″ E) on 10/29/2015 and at Baie d'Authie, France (50° 22′ 17.22″ N, 1° 35′ 4.8″ E) on 11/15/2015. Bivalves were then dissected, digested, and filtered using the method of Dehaut et al. [35]. Particles resembling plastic found in bivalves were extracted under a stereomicroscope using tweezers and submitted to μ-Raman identification using an LabRam HR800 (HORIBA Scientific, Villeneuve d'Ascq, France) following a methodology adapted from Frère et al. [16]. Here, 16 particles from bivalves, previously identified as pigments containing particles, and 10 unknown particles in form of fibers were analyzed. Finally, 24 unknown particles collected in sea surface trawls from the bay of Brest, as described by Frère et al. [38], were used for identification by Py-GC/MS.

Identification by pyrolysis-GC/MS

In total, 60 particles with no previous polymer identification were analyzed. For Py-GC/MS, a piece of each particle was cut to the smallest size possible and prepared as indicated in section 0. Pyrolysis-GC/MS was realized as described above (cf. 0). Results will be present and discuss according to the following categories: pigments containing particles, fibers, and other particles.

Statistical analyses

All statistical analyses with an exception for RSD calculation were performed using R (3.4.0) [39]. For method optimization, including verification of estimated size of microspheres used, normality and homoscedasticity of the distribution hypothesis were carefully verified before performing ANOVA. Assuming one of the hypothesis was not verified, a Kruskal-Wallis test was carried out. Kruskal-Wallis tests were followed by a conservative post hoc test using Fisher's least significant difference (LSD) criterion and Bonferroni correction. Post hoc tests were performed using the agricolae package (1.2-7) [40]. All results are expressed as a mean ± 2 standard error (S.E), representing the 95% confidence interval (95% CI). Differences were considered significant when p value< 0.05. On bar charts, two different letters illustrate significantly different value with a 95% CI.

Results and discussion

All procedural blank, i.e., analysis cup without sample, presented no sign of contamination by pyrolytic products of synthetic polymers.

Method optimization

Pyrolysis temperature

PE microspheres size (204 to 214 μm) used for optimizing the pyrolysis temperature were not significantly different for each tested temperatures (one-way ANOVA, $p > 0.05$). Pyrolysis temperature (500, 600, 700, and 800 °C) had a significant impact on the peaks areas of PE (Fig. 1). On the one hand, for the eight characteristic compounds of PE, peak areas rise when the pyrolysis temperature increases from 500 to 700 °C but on the other hand at 800 °C, peak areas slightly decreased (Fig. 1). Moreover, significant difference of areas was recorded for characteristic compounds of PE (Kruskal-Wallis, $p < 0.05$). Areas were significantly higher at 700 °C in

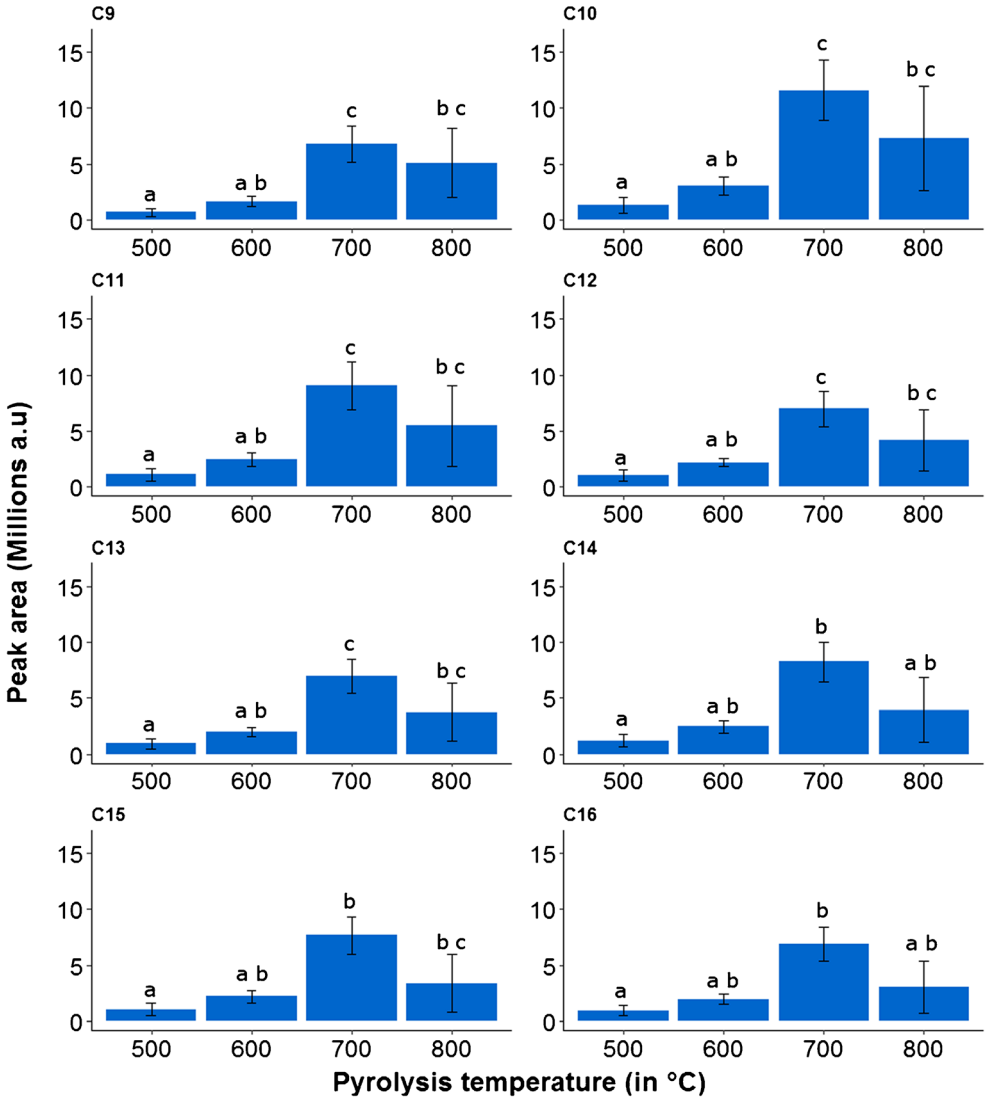

Fig. 1 Peak areas (arbitrary unit) depending on the pyrolysis temperature (in °C) for eight characteristic compounds of PE. Values as expressed as mean ± 95% confidence interval. Letters correspond to the differences after post hoc test using Fisher's least significant difference with Bonferroni correction. C9: 1-Nonene; C10: 1-Decene; C11: 1-Undecene; C12: 1-Dodecene; C13: 1-Tridecene; C14: 1-Tetradecene; C15: 1-Pentadecene; C16: 1-Hexadecene

comparison with areas at 500 °C (Kruskal-Wallis followed by post hoc, $p < 0.05$, Fig. 1). Significant differences between areas at 600 and 700 °C were observed for 1-Nonene, 1-Decene, 1-Undecene, 1-Dodecene, and 1-Tridecene (Kruskal-Wallis followed by post hoc, $p < 0.05$, Fig. 1). However, no significant difference was observed between 500 and 600 °C, between 700 and 800 °C, and between 600 and 800 °C for all 8 characteristic compounds (Kruskal-Wallis followed by post hoc, $p < 0.05$, Fig. 1). At 800 °C, pyrograms of PE microspheres were not all typical with the presence of unknown compounds at the beginning of the pyrogram which lead to identification with a percentage below 80% (see ESM Fig. S9). As 700 °C demonstrated higher areas for characteristic compounds of PE with typical and clearly identified pyrograms, optimal pyrolysis was then set at 700 °C.

Regarding the literature, studies generally used a pyrolysis temperature of 700 °C [19–21, 23, 31, 33] while others used lower temperature such as 550 °C [24], 590 °C [22], 600 °C [32, 35], or 650 °C [25]. As presented in this work, pyrolysis temperature had a clear impact on the signal of the pyrolytic products of PE and could potentially impact identification for small particles. Additionally, pyrolysis at a temperature greater than or equal to 800 °C had a negative effect on PE pyrolytic products. Indeed, the signal was decreased and the polymer identification was not possible with our software due to the presence of a large interfering peak at the beginning of the pyrogram (see ESM Fig. S9). Moreover, as indicated by Kusch [33], pyrolysis temperature could also impact the generated pyrolysis products. Here, for PC, PET, and uPVC, some pyrolysis products were different from those recorded with the initial Py-GC/MS method [35] and from a reference book [32]. Such differences could prevent identification of these polymers as many libraries were obtained after pyrolysis at 600 °C. However, the use of our own database create with pyrolysis temperature set at 700 °C allows accurate polymer identification.

GC oven temperature program

PE microspheres size (197 to 226 μm) used for the optimization of the GC oven temperature program was not significantly different for each tested conditions (one-way ANOVA, $p > 0.05$). For all characteristic compounds of PE and for the three GC oven temperature programs, resolution was above 1.5 (see ESM Fig. S10) which is acceptable [41]. Significant differences in resolution were observed for all peaks of PE (Kruskal-Wallis, $p < 0.01$) depending on the used GC oven temperature program. Moreover, program 2 demonstrated higher resolution in comparison with program 0 and 1 (Kruskal-Wallis followed by Fisher's LSD with Bonferroni correction, $p < 0.05$, see ESM Fig. S10). Here, resolution and peak separation was higher when ramping temperature decrease. Higher peak resolution could be useful for manual identification of peaks, if primary attempt using F-Search software is not conclusive. Program 2 was then applied to perform separation of pyrolysis compounds using the GC system.

Injector temperature and split ratio

PS (110 to 136 μm) and PE (188 to 223 μm) microspheres size used for the optimization on split ratio and injection temperature were not significantly different for each tested conditions (one-way ANOVA, $p > 0.05$). For all characteristic compounds of PE, areas significantly decreased with the increase of split ratio (Kruskal-Wallis followed post hoc, $p < 0.05$, Fig. 2). Moreover, no significant difference in peaks areas were observed at split ratio of 20 and 50 depending on the injector temperature used (Kruskal-Wallis, $p > 0.05$). However, it should be noticed that significant differences between injection at 280, 300, and 320 °C were observed using a split ratio of 5 for all characteristic compounds (Kruskal-Wallis followed by post hoc, $p < 0.05$, Fig. 2). Indeed, with the exception of 1-Nonene, the highest peak areas were obtained when injector temperature was set at 300 °C with a split ratio of 5 (Fig. 2).

For PS, as for PE, increasing split ratio decreased peak areas (Kruskal-Wallis, $p < 0.01$, see ESM Fig. S11). For styrene, at a split ratio of 5, areas were significantly different between 320 °C and the other temperatures (Kruskal-Wallis followed by post hoc, $p < 0.05$, see ESM Fig. S11) and at a split ratio of 20, areas were significantly different between 280 and 320 °C (Kruskal-Wallis followed by post hoc, $p < 0.05$, see ESM Fig. S11). However, no significant difference was observed for area values at a split ratio of 50 between injector temperatures (Kruskal-Wallis, $p < 0.05$). No significant difference was observed for styrene dimer areas between injector temperatures at each split ratio (Kruskal-Wallis, $p > 0.05$).

As split ratio is inversely related to the amounts of sample entering the column, such results were expected. Generally, studies using Py-GC/MS to identify MP used low split ratio to increase analyte signal. Indeed, splitless mode was used for injection by several authors [19–21, 24] while split ratio of 10 [25] or 15 [22] was used by other authors. In several works, split ratio was adapted depending on the weight of the particle to identify [24, 31]. Indeed, Ter Halle et al. [31] used a split ratio of 5 for nanoplastics (25 mg of lyophilizate), 10 for micrometric plastic (particle on filter) and 100 for meso and microplastics and commercial plastics (approximately 10 μg). In addition, in their work, Hendrickson et al. [24] used the splitless mode for particles < 20 μg and a split ratio of 100 for particles > 20 μg. In other studies, few or no information are available on the size or the weight of MP used for pyrolysis [19, 21, 22, 25]. Here, split ratios tested were between 5 and 50 to be around the split ratio used in our previous work [35] and in order to obtain area for PE characteristic peak above a million of arbitrary unit allowing correct identification using the software. With this optimized Py-GC/MS method, split ratio should also be adapted depending on the weight of particles. Indeed, for unknown particles smaller than 5 μg a split ratio of 5 should be used and for particles heavier than 5 μg, split ratio should be set at 20. Moreover, injector temperature of 300 °C in combination with split ratio of 5 had a significant effect on peaks areas for all PE's peaks and for styrene from PS (Fig. 2 and see ESM Fig. S11) which could be important to detect small particles. Here, an injection temperature set at 300 °C was chosen for performance assessment purpose.

Globally, method optimization is an important step for the detection and then the identification of MP using Py-GC/MS. Indeed, the higher the signal will be, the higher the probability of identification will be but mass spectrum saturation should be avoided to ensure proper identification. Moreover, MP signal tends to increase with an increasing size of the particle.

Method performance evaluation

Method repeatability and intermediate precision

PE, PMMA, and PS microspheres used for assessing method repeatability and intermediate precision did not display significant difference in sizes (one-way ANOVA or Kruskal-Wallis, $p > 0.05$). Firstly, polymer identifications were, over the 6 weeks period, accurate with similarity percentage all above 90%. Identification was successful in all cases and the method could be considered repeatable within a week and precise over the 6 weeks. Concerning the repeatability RSD, values were below 20% for the characteristic compounds of PE and PMMA and above 20% for characteristic compounds of PS (Table 2). For styrene dimer, highly variable peak areas were recorded for repeatability test. In addition, RSD value above 20% for styrene was due to one repetition that presents peak area 1.5 higher in comparison with other replicates. Then, concerning intermediate precision RSD values were above 20% for all characteristic compounds of PE, PS, and PMMA

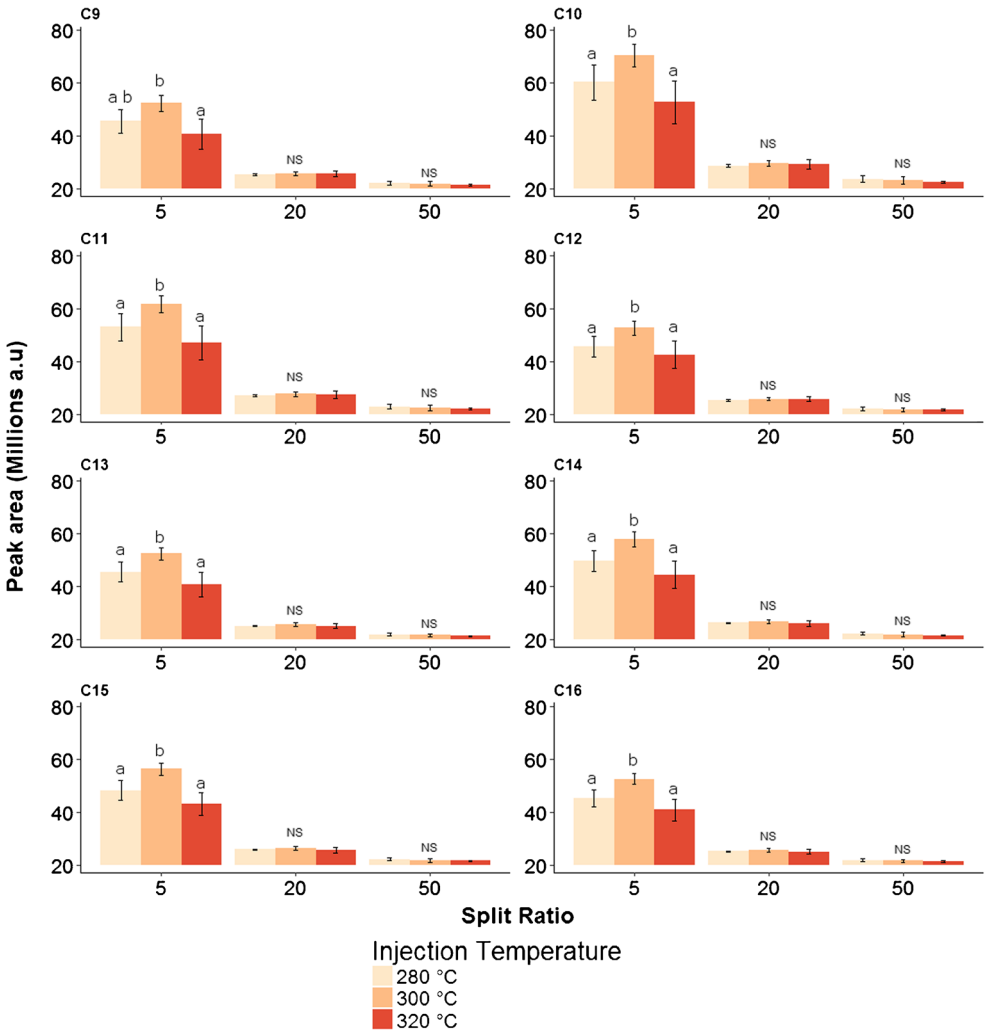

Fig. 2 Peak areas (arbitrary unit) depending on the split ratio and injection temperature for 8 characteristic compounds of PE. Values as expressed as mean ± 95% confidence interval. Letters correspond to the differences after post hoc test using Fisher's least significant difference with Bonferroni correction and NS stand for non-significant. C9: 1-Nonene; C10: 1-Decene; C11: 1-Undecene; C12: 1-Dodecene; C13: 1-Tridecene; C14: 1-Tetradecene; C15: 1-Pentadecene; C16: 1-Hexadecene

(Table 2). Consequently, the method is repeatable for PE and PMMA but not precise over time for all the three tested polymers, regarding quantitative data. Depending on when the analysis was performed, a high variation in peak areas was recorded and thus was responsible for high values of RSD. Indeed, at weeks 1, 3, and 4, areas of characteristic peaks were

Table 2 Relative standard deviation (in %) for method repeatability ($n = 10$) and intermediate precision ($n = 20$) for characteristic compounds of polyethylene, polystyrene, and poly(methyl methacrylate)

Polymer	Characteristic compound	Repeatability RSD (%)	Intermediate precision RSD (%)
PE	1-Nonene	10.67	31.82
	1-Decene	9.91	31.34
	1-Undecene	10.01	31.79
	1-Dodecene	9.55	31.40
	1-Tridecene	9.06	33.11
	1-Tetradecene	8.81	30.22
	1-Pentadecene	8.98	30.88
	1-Hexadecene	9.62	30.76
PS	Styrene	22.47	32.57
	3-Butene-1,3-diyldibenzene (styrene dimer)	48.03	49.69
PMMA	Methyl methacrylate	9.19	24.34

in the same order of magnitude (for an example see ESM Fig. S12). However at week 6, an important diminution of the signal was observed (see ESM Fig. S12) which can cause the high variability in RSD values for method intermediate precision. Finally, despite a decrease over time in peak areas for characteristic compounds of PE, PS, and PMMA, identifications remained exact. This is essential for future use of the optimized Py-GC/MS method to identify MP.

Limit of detection

The estimated LOD was below 1 μg for all tested polymers using the optimized Py-GC/MS (Table 3). Detection of smaller particles of polymers with a few peaks, such as PS or PMMA, could be easier compared to PE which presents numerous pyrolysis products.

To date, identification of isolated MP using Py-GC/MS was successful for particles with a size down to 100 μm [19] and down to 0.4 μg [22]. Here, uPVC demonstrated the highest LOD with 0.592 μg. This could be explained by uPVC fragment form and important density. Indeed, uPVC particles were thick (≈ 310 μm) and long (195 to 220 μm) leading to heavy particles (> 20 μg) due to its important density (1.4 g cm^{-3}) leading to an heavy estimated weight in comparison with other polymers. Globally, polymers with the highest densities, PA-6, PC, or uPVC, have the highest LOD (Table 3). In the present study, estimated weight of the particles used for optimization and performance assessment was below 10 μg with the exception of uPVC particles and was even below 1 μg for some polymers (i.e., PS and PP). Furthermore, in previous works, Py-GC/MS was successfully applied to identify particles weighting 20 μg [24] and below 10 μg [22]. Limit of detection expressed in micrograms was low and demonstrates that this method is applicable to very small and light particles. In addition to LOD in micrometers, theoretical identifiable size (in micrometers) was calculated for MP in form of spheres, fibers, and fragments for all 8 polymer tested in the present study (Table 3). Those theoretical minimal identifiable sizes were calculated using the LOD expressed in mass, polymer density, and Eq. (1–3) (see ESM, weight estimation). For spheres, all identifiable sizes were below 60 μm in diameter, for fibers of 20 μm of diameter length size varied from 9.2 to 366.6 μm and for fragment, all length sizes were below 50 μm (Table 3). Here, these theoretical sizes showed that fibers are the MP form with the longest size identifiable with the optimized Py-GC/MS. Indeed, fibers are long but thin resulting in an important considered size (as the longest size was selected) with a low estimated weight. Moreover, as Py-GC/MS rely on particle weight, it is an important parameter to master in MP research.

MP are commonly defined as plastic particles smaller than 5 mm [7]. However, recently, some studies argue that plastic particles should be described using another parameter [42, 43]. Here, as stated by Simon et al. [43], weight was chosen as an additional parameter to record during MP studies. Indeed, plastics including MP are three-dimensional particles; the description of such particles in accordance with their longest size is problematic and could not be adequate for data interpretations [43]. Actually, it is easy to visualize that there is an important difference in weight for a fiber measuring 500 μm in its longest size with few microns of diameters and a cubic fragment measuring 500 μm for all its sides. This difference in weight could also have different adverse effect when these particles are, for example, ingested by

Table 3 Limit of detection (LOD) for eight common polymer and associate theoretical estimate size of identifiable particle, in the form of sphere, fiber, and fragment

		Theoretical size		
Polymer	LOD (in μg)	Sphere diameter (in μm)[d]	Fiber length (in μm)[d, e]	Fragment length (in μm)[d, f]
PE[a]	0.070	51.7	229.9	28.9
PS[a]	0.003	17.7	9.2	1.2
PMMA[a]	0.029	35.9	77.2	9.7
PA-6[b]	0.110	57.1	309.9	38.9
PP[b]	0.027	38.6	95.5	12.0
PET[b]	0.015	27.4	34.1	4.3
PC[c]	0.116	35.9	77.0	9.7
uPVC[c]	0.592	58.7	366.6	42.3

[a] Polymer used in the form of microspheresside size

[b] Polymer used in the form of filaments

[c] Polymer used in the form of fragments

[d] LOD in size for sphere. Fiber and fragment were calculated based on LOD in weight

[e] Calculation made with a diameter of 20 μm

[f] Calculation made based on a parallelepipoid form with 50 μm as side size

organisms. In addition, plastic emissions to the oceans are estimate in weight [3] and determining MP weight could help for further estimation of MP source and quantities in the Oceans. In the present study, limit of detection of the optimized Py-GC/MS was estimated in micrograms because this technique is dependent on the particle weight and not their size. Moreover, in other studies using thermal analyses, MP could be directly quantified in samples as previously demonstrated [22, 44]. Nevertheless, in the present study, such quantification was not the purpose of the work. For further studies, MP weight should be estimated using weighting if possible or using volume calculation followed by weight estimation using a range of polymer density or using density found in the literature, as done by Simon et al. [43].

However, before being submitted to Py-GC/MS analysis, particles have to be handled with tweezers and placed in an analysis cup. The main limitation with the presented method is the "handibility" of the particles. Below 50 μm, it is very difficult to manipulate the particles as some particles may easily "fly away." Here, the device is not the limiting element whereas the operator is as almost all theoretical identifiable sizes are below 50 μm. Moreover, for application on unknown particles, the highest LOD have to be considered to ensure accurate identification. Consequently and to date, the effective lowest size for plastic identification with this Py-GC/MS method, using particle handling, was evaluated at 50 μm.

Nevertheless, Py-GC/MS has been used to identify nanometric size scale plastic from bulk sample [31]. This approach was made possible as it did not use direct particles handling due to their sizes and because a data statistical treatment was applied after acquisition of pyrograms [31]. If direct handling of particles is not use, Py-GC/MS could be applied to identify smaller plastic particles. Indeed, the use of flow cytometry using sorting [45] could be used to place potential MP in analysis cup. Flow cytometry in combination with a camera and a cell sorter have been used to detect MP [46]. Another technique could be the use of staining techniques like Nile red [47–49] before Py-GC/MS analysis. Indeed, stained particles could be introduced in analysis cup directly with the filter, for example. Moreover, the use of fixing solution to trap MP could also be a solution to isolate this particle and placing them in the analysis cup. However, potential interference of these solutions be carefully controlled before to be employed in routine. With Py-GC/MS, development to isolate particles should be performed to enhance particle handling and to ensure that the device is the only limitation.

Method comparison

Here, particles were collected by hand on a local beach. Particles used to compare identifications between μ-Raman and Py-GC/MS were diverse in shapes and colors. The most common shape was fragments (21), followed by pellets (14), filaments (6), beads (5), and foams (4). Concerning particles color, green was the most common (8), followed by orange (7), blue (7), transparent (6), red (5), yellow (4), white (3), black (3), gray (3), purple (3), and pink (1).

Only 40 out of 50 particles were identified with μ-Raman as plastic particles. From the ten particles not identified, four were identified as pigments containing particles (Cobalt and copper phthalocyanine and Mortoperm blue). Among the 40 identified particles, there were PE (22), PP (11), PS (3), PE-PP copolymer (3), and polyamide (1) (Fig. 3).

The optimized Py-GC/MS method also identified all the 40 particles. Thirty-seven particles (92%) were identified as they were after μ-Raman analysis. Py-GC/MS led to results with a finer identification, two PP particles being identified as PE-PP copolymer. Moreover, the particle identified as polyamide with μ-Raman was identified as a copolymer made of PE, PP, and PA-6 (see ESM Fig. S13). The optimized Py-GC/MS method identified 100% of the 40 previously identified particles with μ-Raman as plastic and demonstrated that this method is reliable for MP identification.

Some particles were not identified with μ-Raman spectroscopy or were identified as pigments. Pigments containing particles identification was also obtained in previous studies on MP from water samples or marine organisms [16, 26–28]. Misidentification could occur for these pigmented particle pigments due to an overlaying of the polymer signal by the additive [11, 50]. Although some pigments are synthetic molecules, it could indicate a synthetic origin but those particles could not be classified as plastic with certainty leading to potential underestimation in field studies. Indeed, some particle containing pigments could simply be colorful paint particles as demonstrated by Imhof et al. [50]. Out of the 6 not identified particles, 3 were discolored pellets. Discoloration indicates that pellets had a higher residence time in the environment [51]. Additionally, Py-GC/MS could also be complementary to FTIR to identified MP in field studies, as recently demonstrated [52]. Indeed, using FTIR polymer signal could be overlap by some plastic additives included and identification could be disturbed [53, 54]. In a recent study, Elert et al. [55] demonstrated that depending on the require information on MP information, i.e., quantification or identification of polymers, the appropriate technique should be used but the authors also indicated that identifications should be used in complementarity. Raman, FTIR, and Py-GC/MS are, to date, the major identification techniques used in MP studies and those techniques are all complementary. Then, the unidentified particles with μ-Raman spectroscopy were analyzed by Py-GC/MS and included in the application section (cf. 0).

Application: identification of unknown particles

On the 60 analyzed particles by Py-GC/MS, 20 (16 particles from bivalves and 4 from beach samples) formerly identified

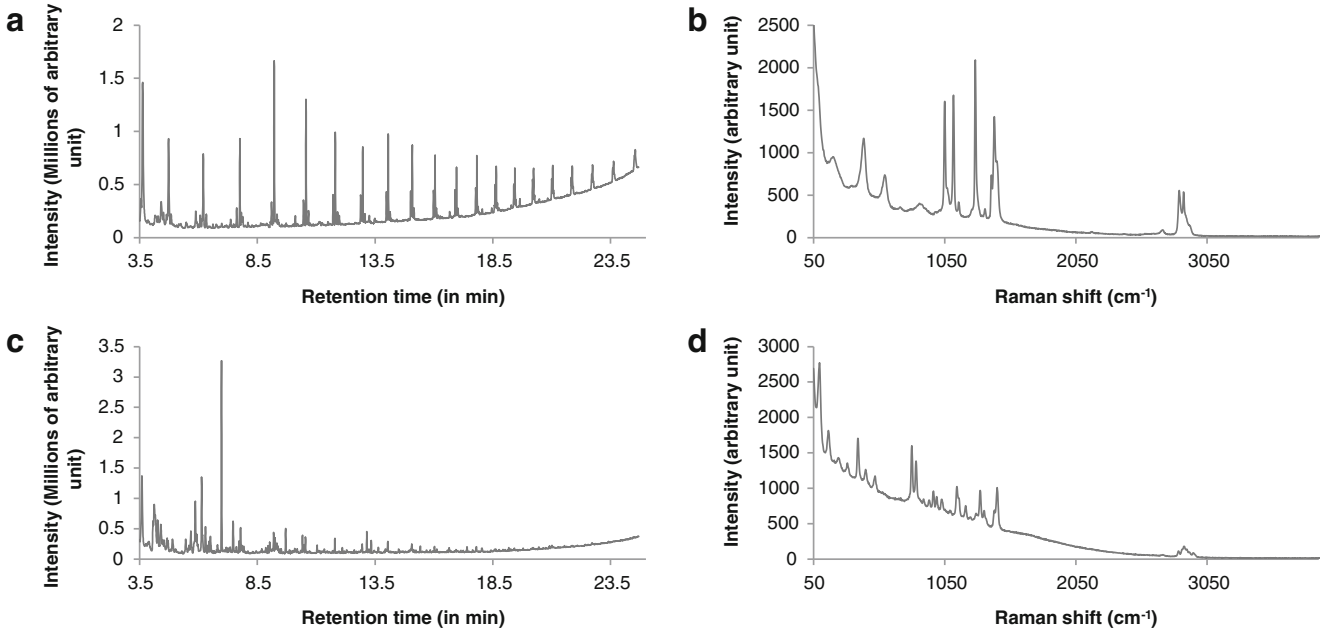

Fig. 3 Pyrograms and Raman spectra acquired at 785 nm obtained from particles collected on a beach used for method comparison. Pyrogram and Raman spectra respectively for a polyethylene MP (**a** and **b**) and a polypropylene MP (**c** and **d**)

as pigment containing particles by μ-Raman were processed by Py-GC/MS. All 20 particles were fragments with blue the dominant color with only one being green. Py-GC/MS identified 14 pigment particles as plastic polymers (70%), 4 pigment particles as plastic polymers with some uncertainty (20%) and 2 particles were not identified (10%, Fig. 4). PS was the most common identified polymer (13 particles out of 14) with one particle identified as a copolymer of PS and PMMA. Moreover, particles identified with uncertainty displayed characteristic compounds of PS but with low intensity. Here, Py-GC/MS identified 70% of particles that were previously identified as pigment containing particles using μ-Raman. Moreover, μ-Raman only identified the presence of the pigments nature as it overlaps with polymer signals, while pyrolysis only allows to identify the native plastic polymer. Despite an effective lowest size of 50 μm, due to handling issue, being 10 to 50 times higher than the lowest size respectively analyzable by FTIR or μ-Raman spectroscopy, respectively, the Py-GC/MS method is still competitive and complementary. Indeed, as it allows (i) the full identification of pigments and some fibers and (ii) could be combined with improved separation methods to retrieve smaller particles. Here, Py-GC/MS could be used as a complementary identification method after μ-Raman spectroscopy.

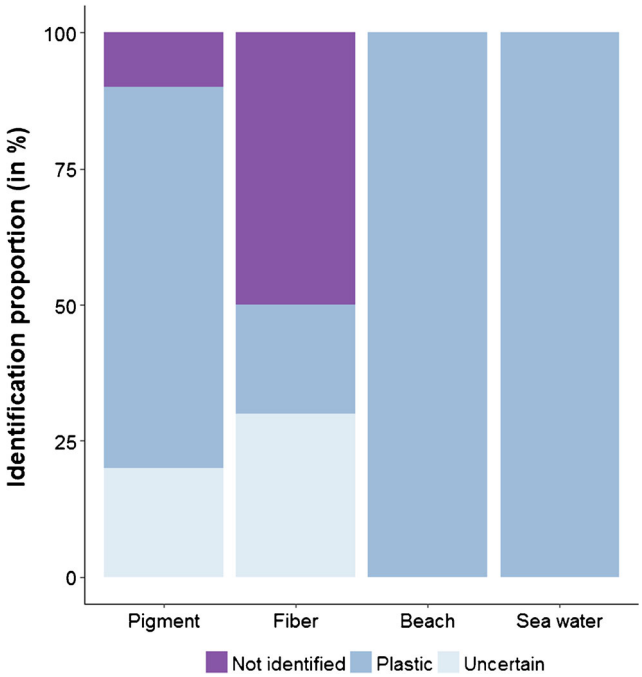

Fig. 4 Sample proportion for each identification class obtained after Py-GC/MS for particles previously identified as pigment ($n = 20$) by μ Raman, fibers ($n = 10$), and particles collected on a beach ($n = 6$) and in surface sea water of the Bay of Brest ($n = 24$). Not identified corresponds to particles with low or no discernible signal, uncertain to identification as plastic with some uncertainty, and plastic to identification with accurate polymer attribution

Out of the 10 fibers extracted from bivalves, 7 were blue, 2 were black, and 1 was red. For fibers, identification was achieved having 2 fibers identified as PE and polyacrylonitrile (PAN). Fibers made of PAN, PE, and potentially PET were identify and such polymer are commonly used in the textile industry [56] and are found in wastewater treatment plants after washing machine [57]. Three fibers were identified as plastic polymer with some uncertainty and 5 fibers were not identified due to low or absent signal (Fig. 4). Uncertain identification for fibers comprised 1 PE and 2 PET. Fibers identification was tough. Indeed, only 20% of the analyzed fibers

were correctly identified. As fibers are long and thin, they are lighter in comparison with fragment. As Py-GC/MS rely more on particle weight than on their size, low weight could result in uncertainty with identifications, as previously observed for fibers in a study conducted by Hendrickson et al. [24]. To improve fibers and small particles identification, a solution could be the use of single ion monitoring (SIM) which target selected ion (m/z) allowing to decrease the LOD.

Out of the 30 other particles collected at sea surface or in beach sediment, fragments (10) were the most common particles followed by foams (6), filaments (5), pellets (4), films (4), and beads (1). Regarding particles color: white was the dominant color (8) followed by blue (6), orange (5), transparent (5), green (3), red (1), black (1), and yellow (1). Particles were all identified as plastic with no uncertainty (Fig. 5); however, it is important to indicate that the particles used in this section were large MP cut (ca. 200 μm) to be introduced in an analysis cup. PE (14) was the most common polymer followed by PP (9) and PS (4). Other polymers including PE-PP copolymer, chlorinated PE (CPE), and acrylonitrile-butadiene-styrene copolymer (ABS) were each found only once. Py-GC/MS provide good identification with similarity percentage above 80%. The differentiation between PS and ABS remained difficult as both polymers are made with styrene which is the major characteristic compounds of their pyrograms [32, 33]. ABS reference presented an interesting characteristic compound: 1-Naphthalenecarbonitrile. This compound was only present in ABS reference pyrogram. Differentiation was made using this compound and tracking it in the pyrogram using its major ion: 153 m/z. Polymers identified, i.e., PE, PP, and PS, are commonly reported on the beach [58] and in sea surface water [38].

Conclusion

The present work described an in-depth optimization of a Py-GC/MS method to identify MP followed by an efficiency assessment of its performance and a comparison with Raman spectroscopic approach. In addition, to evaluate the robustness of the optimized Py-GC/MS method to identify MP, it was applied on samples from different matrices: bivalve, beach, and sea water surface. Optimization demonstrated that increasing pyrolysis temperature up to 700 °C in combination with a split ratio of 5 and an injector temperature set at 300 °C improved signal detection. Then, performance assessment demonstrated that if signal vary over time, such variation had no impact on MP identification. This method is validated on qualitative data but not on quantitative one due to RSD value above 20% for repeatability and intermediate precision.

The optimized Py-GC/MS has some advantages in comparison with other MP identification methods. Firstly, Py-GC/MS is a complementary method to spectroscopy approaches. Indeed, in the present study, Py-GC/MS enable identification of pigment containing particles right after μ-Raman analysis. Moreover, Py-GC/MS identified copolymer like PE-PP or PE-PP-PA6 which could be difficult to identify with μ-Raman without chemometrics approach. Secondly, up to date, Py-GC/MS identification of plastic particles cannot be done below 50 μm (longest size) not because of LOD but due to operator handling issues. A better way, like the introduction of a piece of filter on which particles are into the analysis cup, should be developed in order to avoid this limiting step. However, Py-GC/MS could be used to identify smaller particles, like nanoplastics as already demonstrated. By resolving this handling issue, LOD calculation demonstrated that this method could identify isolated MP weighting below 1 μg. In addition, another strategy that can be considered to lower the LOD for this Py-GC/MS method is the use of SIM. To get identification on MP polluting from both freshwater and marine environment, the use of Py-GC/MS should be better considered as this method prove to be efficient in identifying MP from various matrices. In an effort to standardize the MP analysis workflow, this method could be implemented either on its own or after FTIR or Raman to confirm some identification or to circumvent unsuccessful spectroscopy identification. Finally, MP mass should be evaluated in MP studies to try to standardized leading to better comparison of MP contamination between studies.

Acknowledgments Ludovic Hermabessiere is grateful to the Hauts-de-France Region and ANSES (French Agency for Food, Environmental and Occupational Health & Safety) for the financial support of his PhD. Maria Kazour is financially supported by a PhD fellowship from the National Council for Scientific Research (Lebanon) and Université du Littoral Côte d'Opale (France).

Funding information This paper has been funded by the French National Research Agency (ANR) (ANR-15-CE34-0006-02), as part of the nanoplastics project and also by the French government and the Hauts-de-France Region in the framework of the project CPER 2014-2020 MARCO.

Compliance with ethical standards

Conflict of interest The authors declare that they have no conflict of interest.

References

1. Thompson RC, Swan SH, Moore CJ, vom Saal FS. Our plastic age. Philos Trans R Soc Lond Ser B Biol Sci. 2009;364:1973–6. https://doi.org/10.1098/rstb.2009.0054.
2. PlasticsEurope. Plastics – the Facts 2017: an analysis of European plastics production, demand and waste data. 2018. Available on: http://www.plasticseurope.fr/Document/plastics%2D%2D-the-facts-2017.aspx?FolID=2, Accessed on: 01/29/2018.
3. Jambeck JR, Geyer R, Wilcox C, Siegler TR, Perryman M, Andrady A, et al. Plastic waste inputs from land into the ocean. Science. 2015;347:768–71. https://doi.org/10.1126/science.1260352.

4. Cózar A, Echevarría F, González-Gordillo JI, Irigoien X, Úbeda B, Hernández-León S, et al. Plastic debris in the open ocean. Proc Natl Acad Sci. 2014;111:10239–44. https://doi.org/10.1073/pnas.1314705111.
5. Eriksen M, Lebreton LC, Carson HS, Thiel M, Moore CJ, Borerro JC, et al. Plastic pollution in the world's oceans: more than 5 trillion plastic pieces weighing over 250,000 tons afloat at sea. PLoS One. 2014;9:e111913. https://doi.org/10.1371/journal.pone.0111913.
6. van Sebille E, Wilcox C, Lebreton L, Maximenko N, Hardesty BD, van Franeker JA, et al. A global inventory of small floating plastic debris. Environ Res Lett. 2015;10:124006. https://doi.org/10.1088/1748-9326/10/12/124006.
7. Arthur, C., J. Baker, H. Bamford. International research workshop on the occurrence, effects, and fate of microplastic marine debris. NOAA Technical Memorandum NOS-OR&R-30; 2009.
8. Li WC, Tse HF, Fok L. Plastic waste in the marine environment: a review of sources, occurrence and effects. Sci Total Environ. 2016;566–567:333–49. https://doi.org/10.1016/j.scitotenv.2016.05.084.
9. Horton AA, Walton A, Spurgeon DJ, Lahive E, Svendsen C. Microplastics in freshwater and terrestrial environments: evaluating the current understanding to identify the knowledge gaps and future research priorities. Sci Total Environ. 2017;586:127–41. https://doi.org/10.1016/j.scitotenv.2017.01.190.
10. Imhof HK, Schmid J, Niessner R, Ivleva NP, Laforsch C. A novel, highly efficient method for the separation and quantification of plastic particles in sediments of aquatic environments. Limnol Oceanogr Methods. 2012;10:524–37. https://doi.org/10.4319/lom.2012.10.524.
11. Lenz R, Enders K, Stedmon CA, Mackenzie DMA, Nielsen TG. A critical assessment of visual identification of marine microplastic using Raman spectroscopy for analysis improvement. Mar Pollut Bull. 2015;100:82–91. https://doi.org/10.1016/j.marpolbul.2015.09.026.
12. Shim WJ, Hong SH, Eo SE. Identification methods in microplastic analysis: a review. Anal Methods. 2017;9:1384–91. https://doi.org/10.1039/C6AY02558G.
13. CAMPUS. 2018. Available on: https://www.campusplastics.com/campus/list. Accessed on: 01/26/2018.
14. Remy F, Collard F, Gilbert B, Compère P, Eppe G, Lepoint G. When microplastic is not plastic: the ingestion of artificial cellulose fibers by macrofauna living in Seagrass Macrophytodetritus. Environ Sci Technol. 2015;49:11158–66. https://doi.org/10.1021/acs.est.5b02005.
15. Rocha-Santos T, Duarte AC. A critical overview of the analytical approaches to the occurrence, the fate and the behavior of microplastics in the environment. TrAC. 2015;65:47–53. https://doi.org/10.1016/j.trac.2014.10.011.
16. Frère L, Paul-Pont I, Moreau J, Soudant P, Lambert C, Huvet A, et al. A semi-automated Raman micro-spectroscopy method for morphological and chemical characterizations of microplastic litter. Mar Pollut Bull. 2016;113:461–8. https://doi.org/10.1016/j.marpolbul.2016.10.051.
17. Oßmann BE, Sarau G, Schmitt SW, Holtmannspötter H, Christiansen SH, Dicke W. Development of an optimal filter substrate for the identification of small microplastic particles in food by micro-Raman spectroscopy. Anal Bioanal Chem. 2017;409:4099–109. https://doi.org/10.1007/s00216-017-0358-y.
18. Phuong NN, Zalouk-Vergnoux A, Kamari A, Mouneyrac C, Amiard F, Poirier L, Lagarde F. Quantification and characterization of microplastics in blue mussels (*Mytilus edulis*): protocol setup and preliminary data on the contamination of the French Atlantic coast. Environ Sci Pollut Res Int. 2017:1–10. https://doi.org/10.1007/s11356-017-8862-3.
19. Dekiff JH, Remy D, Klasmeier J, Fries E. Occurrence and spatial distribution of microplastics in sediments from Norderney. Environ Pollut. 2014;186:248–56. https://doi.org/10.1016/j.envpol.2013.11.019.
20. Fries E, Dekiff JH, Willmeyer J, Nuelle M-T, Ebert M, Remy D. Identification of polymer types and additives in marine microplastic particles using pyrolysis-GC/MS and scanning electron microscopy. Environ Sci Process Impacts. 2013;15:1949–56. https://doi.org/10.1039/C3EM00214D.
21. Nuelle M-T, Dekiff JH, Remy D, Fries E. A new analytical approach for monitoring microplastics in marine sediments. Environ Pollut. 2014;184:161–9. https://doi.org/10.1016/j.envpol.2013.07.027.
22. Fischer M, Scholz-Böttcher BM. Simultaneous trace identification and quantification of common types of microplastics in environmental samples by pyrolysis-gas chromatography–mass spectrometry. Environ Sci Technol. 2017;51:5052–60. https://doi.org/10.1021/acs.est.6b06362.
23. Fabbri D, Tartari D, Trombini C. Analysis of poly(vinyl chloride) and other polymers in sediments and suspended matter of a coastal lagoon by pyrolysis-gas chromatography-mass spectrometry. Anal Chim Acta. 2000;413:3–11. https://doi.org/10.1016/S0003-2670(00)00766-2.
24. Hendrickson E, Minor EC, Schreiner K. Microplastic abundance and composition in western Lake Superior as determined via microscopy, Pyr-GC/MS, and FTIR. Environ Sci Technol. 2018;52:1787–96. https://doi.org/10.1021/acs.est.7b05829.
25. Ceccarini A, Corti A, Erba F, Modugno F, La Nasa J, Bianchi S, et al. The hidden microplastics. New insights and figures from the thorough separation and characterization of microplastics and of their degradation by-products in coastal sediments. Environ Sci Technol. 2018; https://doi.org/10.1021/acs.est.8b01487.
26. Van Cauwenberghe L, Claessens M, Vandegehuchte MB, Janssen CR. Microplastics are taken up by mussels (*Mytilus edulis*) and lugworms (*Arenicola marina*) living in natural habitats. Environ Pollut. 2015;199:10–7. https://doi.org/10.1016/j.envpol.2015.01.008.
27. Van Cauwenberghe L, Janssen CR. Microplastics in bivalves cultured for human consumption. Environ Pollut. 2014;193:65–70. https://doi.org/10.1016/j.envpol.2014.06.010.
28. Schymanski D, Goldbeck C, Humpf H-U, Fürst P. Analysis of microplastics in water by micro-Raman spectroscopy: release of plastic particles from different packaging into mineral water. Water Res. 2018;129:154–62. https://doi.org/10.1016/j.watres.2017.11.011.
29. Li J, Liu H, Paul Chen J. Microplastics in freshwater systems: a review on occurrence, environmental effects, and methods for microplastics detection. Water Res. 2018;137:362–74. https://doi.org/10.1016/j.watres.2017.12.056.
30. Ivleva NP, Wiesheu AC, Niessner R. Microplastic in aquatic ecosystems. Angew Chem Int Ed. 2016;56:1720–39. https://doi.org/10.1002/anie.201606957.
31. Ter Halle A, Jeanneau L, Martignac M, Jardé E, Pedrono B, Brach L, et al. Nanoplastic in the North Atlantic subtropical gyre. Environ Sci Technol. 2017;51:13689–97. https://doi.org/10.1021/acs.est.7b03667.
32. Tsuge S, Ohtani H, Watanabe C. Pyrolysis-GC/MS data book of synthetic polymers. Elsevier; 2011. p 390.
33. Kusch P. Application of pyrolysis-gas chromatography/mass spectrometry (Py-GC/MS), in characterization and analysis of microplastics. In: Rocha-Santos T, Duarte A, editors. Elsevier; 2016. p 306.
34. van Den Dool H, Kratz PD. A generalization of the retention index system including linear temperature programmed gas—liquid partition chromatography. J Chromatogr A. 1963;11:463–71. https://doi.org/10.1016/S0021-9673(01)80947-X.
35. Dehaut A, Cassone A-L, Frère L, Hermabessiere L, Himber C, Rinnert E, et al. Microplastics in seafood: benchmark protocol for their extraction and characterization. Environ Pollut. 2016;215:223–33. https://doi.org/10.1016/j.envpol.2016.05.018.
36. International Organization for Standardization (ISO), 5725-3: 1994. Accuracy (trueness and precision) of measurement methods and results-part 3: intermediate measures of the precision of a standard measurement method. Geneva: International Organization for Standardization; 1994.
37. Caporal-Gautier J, Nivet JM, Algranti P, Guilloteau M, Histe M, Lallier M, et al. Guide de validation analytique: rapport d'une

commission SFSTP I: méthodologie. STP Pharma Pratiques. 1992;2:205–26.
38. Frère L, Paul-Pont I, Rinnert E, Petton S, Jaffré J, Bihannic I, et al. Influence of environmental and anthropogenic factors on the composition, concentration and spatial distribution of microplastics: a case study of the bay of Brest (Brittany, France). Environ Pollut. 2017;225:211–22. https://doi.org/10.1016/j.envpol.2017.03.023.
39. R Core Team. R: A language and environment for statistical computing. Vienna, Austria; 2014. 2015. Available on: http://www.R-project.org, Accessed on: 10/15/2015.
40. De Mendiburu F. Agricolae: statistical procedures for agricultural research. 2014. R package version.
41. McGuffin VL. Theory of chromatography, in Journal of Chromatography Library. Elsevier; 2004. p. 1–93.
42. Filella M. Questions of size and numbers in environmental research on microplastics: methodological and conceptual aspects. Environ Chem. 2015;12:527–38. https://doi.org/10.1071/EN15012.
43. Simon M, van Alst N, Vollertsen J. Quantification of microplastic mass and removal rates at wastewater treatment plants applying focal plane array (FPA)-based Fourier transform infrared (FT-IR) imaging. Water Res. 2018;142:1–9. https://doi.org/10.1016/j.watres.2018.05.019.
44. Dümichen E, Barthel A-K, Braun U, Bannick CG, Brand K, Jekel M, et al. Analysis of polyethylene microplastics in environmental samples, using a thermal decomposition method. Water Res. 2015;85:451–7. https://doi.org/10.1016/j.watres.2015.09.002.
45. Ibrahim SF, van den Engh G. Flow cytometry and cell sorting, in cell separation: fundamentals, analytical and preparative methods. In: Kumar A, Galaev IY, Mattiasson B, editors. Berlin, Heidelberg: Springer Berlin Heidelberg; 2007. p. 19–39.
46. Sgier L, Freimann R, Zupanic A, Kroll A. Flow cytometry combined with viSNE for the analysis of microbial biofilms and detection of microplastics. Nat Commun. 2016;7:11587. https://doi.org/10.1038/ncomms11587.
47. Shim WJ, Song YK, Hong SH, Jang M. Identification and quantification of microplastics using Nile Red staining. Mar Pollut Bull. 2016;113:469–76. https://doi.org/10.1016/j.marpolbul.2016.10.049.
48. Maes T, Jessop R, Wellner N, Haupt K, Mayes AG. A rapid-screening approach to detect and quantify microplastics based on fluorescent tagging with Nile Red. Sci Rep. 2017;7:44501. https://doi.org/10.1038/srep44501.
49. Erni-Cassola G, Gibson MI, Thompson RC, Christie-Oleza JA. Lost, but found with Nile Red: a novel method for detecting and quantifying small microplastics (1 mm to 20 μm) in environmental samples. Environ Sci Technol. 2017;51:13641–8. https://doi.org/10.1021/acs.est.7b04512.
50. Imhof HK, Laforsch C, Wiesheu AC, Schmid J, Anger PM, Niessner R, et al. Pigments and plastic in limnetic ecosystems: a qualitative and quantitative study on microparticles of different size classes. Water Res. 2016;98:64–74. https://doi.org/10.1016/j.watres.2016.03.015.
51. Endo S, Takizawa R, Okuda K, Takada H, Chiba K, Kanehiro H, et al. Concentration of polychlorinated biphenyls (PCBs) in beached resin pellets: variability among individual particles and regional differences. Mar Pollut Bull. 2005;50:1103–14. https://doi.org/10.1016/j.marpolbul.2005.04.030.
52. Käppler A, Fischer M, Scholz-Böttcher BM, Oberbeckmann S, Labrenz M, Fischer D, et al. Comparison of μ-ATR-FTIR spectroscopy and py-GCMS as identification tools for microplastic particles and fibers isolated from river sediments. Anal Bioanal Chem. 2018; https://doi.org/10.1007/s00216-018-1185-5.
53. Tabb DL, Koenig JL. Fourier transform infrared study of plasticized and unplasticized poly(vinyl chloride). Macromolecules. 1975;8:929–34. https://doi.org/10.1021/ma60048a043.
54. González N, Fernández-Berridi MJ. Application of Fourier transform infrared spectroscopy in the study of interactions between PVC and plasticizers: PVC/plasticizer compatibility versus chemical structure of plasticizer. J Appl Polym Sci. 2006;101:1731–7. https://doi.org/10.1002/app.23381.
55. Elert AM, Becker R, Duemichen E, Eisentraut P, Falkenhagen J, Sturm H, et al. Comparison of different methods for MP detection: what can we learn from them, and why asking the right question before measurements matters? Environ Pollut. 2017;231:1256–64. https://doi.org/10.1016/j.envpol.2017.08.074.
56. Napper IE, Thompson RC. Release of synthetic microplastic plastic fibres from domestic washing machines: effects of fabric type and washing conditions. Mar Pollut Bull. 2016;112:39–45. https://doi.org/10.1016/j.marpolbul.2016.09.025.
57. Browne MA, Crump P, Niven SJ, Teuten E, Tonkin A, Galloway T, et al. Accumulation of microplastic on shorelines worldwide: sources and sinks. Environ Sci Technol. 2011;45:9175–9. https://doi.org/10.1021/es201811s.
58. Lots FAE, Behrens P, Vijver MG, Horton AA, Bosker T. A large-scale investigation of microplastic contamination: abundance and characteristics of microplastics in European beach sediment. Mar Pollut Bull. 2017;123:219–26. https://doi.org/10.1016/j.marpolbul.2017.08.057.